(35) Ohta, T.; Termato, A.; Fujita, H. *Polym. J.* **1976**, *8*, 281.
(36) σ values of PBLG, PHPG, and PHEG are 9.0×10^{-5}, 3.2×10^{-4}, and $(1.5\text{–}4.4) \times 10^{-3}$.[33-35]
(37) Flory, P. J. *Macromolecules* **1974**, *7*, 381.
(38) Conrad, J. C.; Flory, P. J. *Macromolecules* **1976**, *9*, 41.
(39) Schimmel, P. R.; Flory, P. J. *Proc. Natl. Acad. Sci. U.S.A.* **1967**, *58*, 52. (T_c) of L-proline in this reference suffices for the model of the extended coil structure, but cannot give a correct unperturbed dimension of poly(L-proline); see: Tanaka, S.; Scheraga, H. A. *Macromolecules* **1975**, *8*, 623.

Investigation of the Chain Conformation in Uniaxially Stretched Poly(dimethylsiloxane) Networks by Small-Angle Neutron Scattering

Michel Beltzung, Claude Picot, and Jean Herz*

Centre de Recherches sur les Macromolécules (CNRS), 67083 Strasbourg, France.
Received May 19, 1983

ABSTRACT: The behavior of network chains in dry poly(dimethylsiloxane) networks submitted to uniaxial extension was investigated by small-angle neutron scattering. The measurements were carried out on "end-linked" networks. The experimental results were compared with those expected on the basis of the models proposed by the classical theories of rubber elasticity, but the observed behavior at the level of the elastic chain cannot be interpreted within the framework of a unique model. An interpretation of the chain behavior, taking into account a rearrangement of cross-link positions upon deformation, is proposed.

I. Introduction

In spite of very intensive theoretical and experimental investigations, many questions concerning the behavior of elastic chains in rubber networks remain open or are still subject to controversy. Therefore the study of the network behavior at a molecular level in relation to the structural characteristics of the system is of major interest.

A previous article was devoted to an investigation by small-angle neutron scattering (SANS) of poly(dimethylsiloxane) (PDMS) networks in the dry undeformed state;[1] it was shown that upon cross-linking in the bulk by an end-linking process involving a polymer precursor, the chain dimensions remain unchanged. On the other hand, no memory effect or supercoiling of the elastic chains could be observed.

A macroscopic deformation of the network, either by swelling in a solvent or by mechanical constraint, induces a displacement of the cross-links and thus gives rise to a deformation of the elastic chains attached to the latter. An investigation by SANS of the behavior of the elastic chains in PDMS networks upon swelling in a thermodynamically good solvent has been published recently.[2]

The present article is focused on a study of dry PDMS networks submitted to uniaxial extension. Again, SANS is a powerful technique to characterize the deformation of the elastic chains that results from a macroscopic deformation of the system. The scattering experiments were carried out on samples on which the stress–strain behavior was determined simultaneously.

II. Theory

The deformation ratio of a network submitted to a uniaxial extension parallel to the Oz axis is defined by $\lambda_z = \lambda = L/L_i$, where L and L_i are the lengths of the deformed and undeformed sample. Generally, one assumes that deformation occurs at constant volume: $\lambda_x = \lambda_y = \lambda_z^{-1/2}$. The corresponding elastic force is given by

$$F = \left(\frac{\delta A_{el}}{\delta L}\right)_{T,v} = \left(\frac{\delta A_{el}}{\delta \lambda}\right)_{T,v} \frac{1}{L_i} \tag{1}$$

A_{el} is the elastic free energy of the system.

In the earliest theories of rubber elasticity[3-7] the cross-links were considered to be firmly embedded in the elastomeric polymer matrix. This implies that in the deformed sample the displacement of these cross-links is affine in the macroscopic deformation.

The elastic energy was calculated in the case of Gaussian chains.[8] To define the elastic free energy, a reference state was considered, in which the mean square end-to-end distance of the elastic chains is the same as that of the unperturbed free chains. According to experiments reported earlier,[1] this can be considered to be true for undeformed dry networks. Under these hypotheses the stress σ and the shear modulus G are given by

$$\sigma = \frac{F}{S_i} = \nu RT(\lambda - \lambda^{-2}) \tag{2}$$

$$G = \lim_{\lambda \to 1}\left(\frac{\sigma}{\lambda - \lambda^{-2}}\right) = \nu RT \tag{3}$$

where S_i is the cross section of the undeformed sample, ν the number of network chains per unit volume, R the gas constant, and T the absolute temperature.

Another approach is based on the "phantom network" model of James and Guth.[9,10] These authors supposed that the network chains can move freely without any restriction due to neighboring chains. The elastic chains merely transmit the forces exerted upon the junctions. The chains are assumed to follow Gaussian statistics. Such a phantom network can be characterized as follows:[9-11] (i) the mean positions of the cross-links are defined by the macroscopic dimensions of the sample, (ii) the displacements of these mean positions are affine in the macroscopic deformation, and (iii) the fluctuations of the cross-links from their mean positions are Gaussian and their amplitude is independent of the deformation applied. Graessley[12] has calculated the elastic free energy and the strain corresponding to a deformation ratio λ:

$$\sigma = (\nu - \mu)RT(\lambda - \lambda^{-2}) \tag{4}$$

where μ represents the number of cross-links per unit volume. The shear modulus of a phantom network is thus

$$G = (\nu - \mu)RT \tag{5}$$

This means that for a tetrafunctional network (where $\nu/\mu = 2$) $G = {}^1/_2\nu RT$, half the shear modulus calculated in the

0024-9297/84/2217-0663$01.50/0

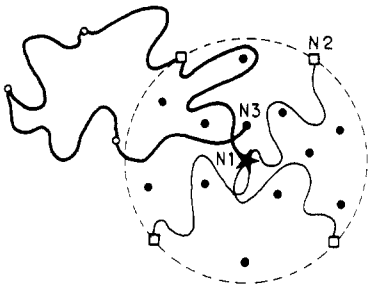

Figure 1. Scheme of a dry network. The star represents a reference cross-link (N_1). The sphere has a radius equal to the end-to-end distance of the elementary elastic chain. The squares refer to topological neighboring cross-links (N_2) (directly connected). The points represent spatial first neighbors (N_3).

absence of cross-link fluctuations (junction affine model eq 3).

The real behavior of a network should be intermediate between that of the junction affine and the phantom network models. In fact, the network chains strongly interpenetrate. According to Flory,[13,14] this interpenetration induces a stress upon the junction points, but any contribution of the trapped or the temporary entanglements to the elastic behavior of the networks is denied.

The above theories of rubber elasticity do not allow a plausible interpretation of several recent experimental results:[15,16] it was shown by osmotic deswelling that a network can undergo important macroscopic deformations without any appreciable change in the dimensions of the elastic chains. To explain such a behavior, Bastide[17] suggested a deformation process based upon a molecular rearrangement of the chains. His idea is based on a remark by Flory,[18] according to which the network chains are strongly interpenetrated in the dry state. This induces a distinction between two types of neighboring cross-links around any given cross-link N_1 of the system (Figure 1): (i) the topological first neighbours N_2 linked to N_1 by an elastic chain (there are f topological neighbors if the cross-link functionality is f); and (ii) the spatial first neighbors N_3, which are at a distance smaller than or equal to that of the topological neighbors but not linked directly to N_1.

The number n of spatial neighbors can be calculated easily.[16,17,19] If $\langle r^2 \rangle$ is the mean square end-to-end distance of the elastic chains, all these spatial neighbors to one given cross-link are located within a sphere of radius $\langle r^2 \rangle^{1/2}$, the volume of which is $V = {}^4/_3\pi\langle r^2 \rangle^{3/2}$. For linear Gaussian chains, $\langle r^2 \rangle$ is related to the radius of gyration R_g by the classical expression $\langle r^2 \rangle = 6R_g^2$ and in the case of PDMS to the molecular weight by the experimental relation[1]

$$\langle r^2 \rangle = 6(0.25)^2 M_w$$

The volume occupied by a single chain is $v = (M/\mathcal{N})v_s$, where $\mathcal{N}$ is Avogadro's number and v_s the specific volume of the polymer. Since the number of chains within the volume V is V/v, the total number of cross-links is given by $n = (2/f)(V/v)$ and the ratio of the total number of cross-links to the number of topological neighbors is

$$\frac{n}{f} = \frac{2}{f^2}\frac{V}{v} \tag{6}$$

In the case of PDMS, $n/f = 1.5(M^{0.5})/f^2$. Table I displays the values calculated for PDMS over a molecular weight range 3000–23 000 and functionalities of cross-links $f = 4$ and 6. It follows that in the unswollen networks used in the present investigation the number of spatial neighbors is noticeably larger than that of topological neighbors. This

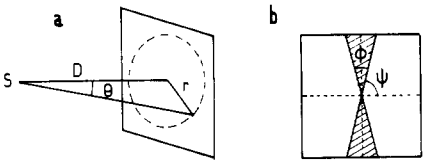

Figure 2. Scheme for analysis of anisotropic small-angle scattering. θ is the scattering angle and D the sample (S)–detector (P) distance. In the frame of the detector, ψ is the azimuthal angle of the sector selected for data analysis (0° and 90°) and ϕ is its aperture (20°).

Table I
Values of the Ratio n/f of the Total Number of Neighbor Cross-Links to the Number of Topological Neighbors

M_n	f	n/f
3 100	4	6.5
6 100	4	9.4
10 500	4	12.2
10 500	6	5.4
23 000	4	17.3
23 000	6	7.7

appears on Bastide's model shown in Figure 1. It indicates schematically that the path that joins two spatial neighbors passes through several other cross-links. This model suggests that in a deformed network the elastic chains linked to two topological neighbors are less deformed than the large path between spatial neighbors. The larger the value of n/f, the more likely the deformation by rearrangement of cross-links and disinterpenetration of network chains.[15]

III. Experimental Section

Samples. PDMS networks containing a known fraction of deuterated elastic chains were prepared as described earlier[1] by an end-linking process involving α,ω-difunctional precursor polymers. The samples were cross-linked in the bulk or in solution at polymer concentrations v_c above 0.5. Functional polymers with molecular weights between 3000 and 25 000 were used. The volume fraction of deuterated network chains in the samples was 0.2 in all cases. Some soluble material was extracted from the gels with toluene. It corresponds mainly to small cyclic species (about 3.6%) always present in the precursor polymers and a very small fraction of unreacted functional precursor (0.3–0.9%).

The uniaxial extension experiments were carried out on small strips of network with dimensions of approximately 40 × 15 × 1.2 mm. These strips were cut out from the swollen samples and dried, very slowly at first, to avoid crack formation, and then under vacuum at 60 °C, to constant weight.

Sample Holder and Stretching Device. The gel strips were held firmly on a sample holder by means of two mobile crossheads. A micrometric screw operates the displacements of the crossheads. This allows stretching of the sample and accurate measurements of its length before and after deformation. The upper crosshead is fixed to a force transducer connected with a measurement bridge (HBM KWS 3.082) and a millivoltmeter (Metrix MX 515). This apparatus can be fit within the SANS device.

Thus the force F applied to the sample and the corresponding deformation ratio $\lambda = L/L_i$ can be measured, and the stress $\sigma = F/S_i$ calculated.

SANS Measurements. The neutron scattering experiments on stretched PDMS networks were carried out on the D17 small-angle scattering spectrometer of the Institute Von Laue-Langevin (Grenoble, France). The values of the momentum transfer $|q| = (4\pi/\lambda) \sin(\theta/2)$ are in the range 10^{-2} to 8×10^{-2} Å^{-1}.

For the analysis of the anisotropy of the samples, two sectors of the bidimensional detector were considered: the first one corresponds to the direction parallel to the stretching axis and the second one to the direction perpendicular to the stretching axis ($\psi = 90°$ and $\psi = 0°$). The width of the sector is characterized by the angle $\phi = 20°$ (Figure 2), which corresponds to the optimal conditions: for lower values of ϕ the accuracy of the measurements

would become poorer; for higher values the intensity measured would contain an increasing contribution of a secondary compound, which cannot be neglected.

As in the case of undeformed isotropic networks,[1] the measurements of the intensity scattered by a partly deuterated system have to be corrected for incoherent scattering and for the counting efficiency of the measuring cells. The incoherent intensity is determined by using an undeuterated undeformed sample. It was checked that the results are identical in the deformed system. It has been established both theoretically and experimentally[20-23] that in the case of melts of identical deuterated and undeuterated chains, the coherent neutron scattering contribution is directly proportional to the intrachain scattering form factor $P(q)$ through the relation

$$I(q) \sim (b_D - b_H)^2 N \varphi_D (1 - \varphi_D) P(q) \quad (7)$$

where b_D and b_H are the coherent scattering lengths per unit volume of the deuterated and undeuterated species, N is the number of chains in the mixture, φ_D is the volume fraction of deuterated compound, and q is the momentum transfer. Recently, it was shown[1] that this expression is valid also in the case of networks containing a high fraction of deuterated elastic chains, thus providing a better precision and an appreciable gain of exposure time for SANS measurements.

It must be noted that eq 7 is no longer valid when a molecular weight mismatch between H and D species exists. In that case, as mentioned in ref 1 and 23, one is led by a Zimm representation in the small-q range to evaluate an apparent mean square radius of gyration $\langle R_g^2 \rangle_{app}$.

$$(P(q))^{-1} \simeq 1 + q^2 \frac{\langle R_g^2 \rangle_{app}}{3} \quad \text{for} \quad q^2 \langle R_g^2 \rangle_{app} \ll 1 \quad (8)$$

As discussed in ref 1, for samples used in the present investigations, $\langle R_g^2 \rangle_{app}$ does not differ, within the limit of experimental error, from the $\langle R_g^2 \rangle_z$ value obtained in the case of exact matching of H and D species.

An equation similar to (8) can also be applied in the anisotropic case. By analyzing the intensities in the directions parallel ($q_\parallel$) and perpendicular ($q_\perp$) to the stretching direction, one obtains the component of the radius of gyration in these two main directions through the relation

$$P_k^{-1}(q) \simeq 1 + q^2 \langle R_g^2 \rangle_k \qquad k = \parallel \text{ or } \perp \quad (8')$$

These two components, $R_{g,\parallel}$ and $R_{g,\perp}$, can also be calculated as a function of the extension ratio λ, considering the theoretical deformation modes: junction affine deformation, phantom network deformation, and affine deformation.

Junction Affine Deformation. The deformation of the elastic chains that is induced by the displacement of the cross-links, affine in the macroscopic deformation, is characterized by the expressions[24,25]

$$\frac{R_{g,\parallel}}{R_{g,i}} = \alpha_\parallel = \left(\frac{\lambda^2 + 1}{2} \right)^{1/2} \quad (9)$$

$$\frac{R_{g,\perp}}{R_{g,i}} = \alpha_\perp = \left(\frac{\lambda + 1}{2\lambda} \right)^{1/2} \quad (10)$$

where $R_{g,i}$ is the component of the radius of gyration of the network chains in the undeformed system.

Phantom Network. Pearson[26] has calculated $\alpha_\parallel$ and $\alpha_\perp$ for a uniaxially stretched phantom network. These values depend upon the functionality of the cross-links:

$$\frac{R_{g,\parallel}}{R_{g,i}} = \alpha_\parallel = \left(\frac{f + 2 + (f-2)\lambda^2}{2f} \right)^{1/2} \quad (11)$$

$$\frac{R_{g,\perp}}{R_{g,i}} = \alpha_\perp = \left(\frac{f + 2 + (f-2)\lambda^{-1}}{2f} \right)^{1/2} \quad (12)$$

Affine Deformation. This model assumes that the deformation of each chain segment is affine in the macroscopic deformation. This means that

$$R_{g,\parallel}/R_{g,i} = \alpha_\parallel = \lambda \quad (13)$$

$$R_{g,\perp}/R_{g,i} = \alpha_\perp = \lambda^{-1/2} \quad (14)$$

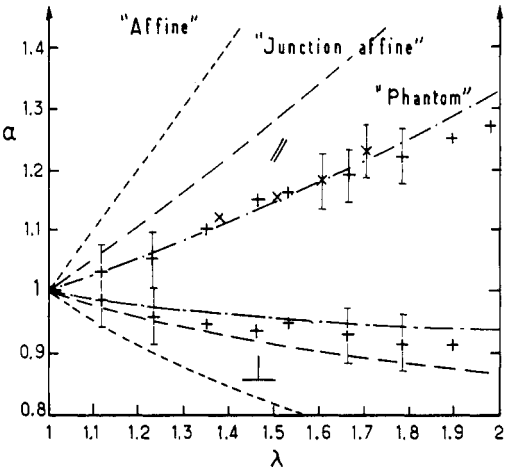

Figure 3. Variation of the molecular deformation α in the direction parallel ($\parallel$) and perpendicular ($\perp$) to the stretching direction. (×) and (+) represent the experimental values obtained for two independent measurements on an identical network (M_n = 9700).

The classical theories of elasticity do not consider this model.

The experimental results can thus be compared with the values calculated according to the above equations (9)–(14). One must add that during stretching, $R_{g,\parallel}$ can reach values that exceed the requirement $q^2 \langle R_g^2 \rangle_{app} \ll 1$. In fact, due to the polydispersity of the labeled species ($M_w/M_n \sim 1.6$), this requirement is less drastic, a suitable linearity of the Zimm representation being obtained up to $qR_g \sim 4$.

Accuracy and Reproducibility of the Measurements. On Figure 3 the experimental values of $\alpha_\parallel$ and $\alpha_\perp$ are plotted vs. λ for two samples originating from the same network. (Molecular weight of elastic chains M_n = 9 700.) The precision of the value of the radius of gyration measured cannot be estimated directly. However, it can be characterized by the relative uncertainty $\Delta R_g/R_g$, which reflects the dispersion of the experimental points on the Zimm plots, $c/I = f(q^2)$, from which $R_{g,i}$, $R_{g,\parallel}$, and $R_{g,\perp}$ are extracted. This leads to an estimation of $\Delta\alpha/\alpha$ of approximately 5%. It follows that the values that correspond to small extension ratios ($\lambda \to 1$) have to be accounted for with much care (Figure 3).

The relative error of the deformation ratio is rather low: $\Delta\lambda/\lambda \approx 0.2\%$.

Thus, within the limits of experimental accuracy, the results obtained for both samples can be considered as identical. The dotted curves in Figure 3 correspond to the calculated variation of α vs. λ according to the three theoretical models mentioned above. The experimental points lie on the curve predicted by the phantom network model.

Simultaneous measurements of the stress applied and of the resulting deformation allow the determination of the elastic modulus. Another advantage of this procedure is that an accidental slipping of the sample in the crossheads can be detected immediately. It was checked that the measurements of the strain are correct within a margin below 5%.

In the case of small deformation ratios the moduli were determined by separate measurements using the Mooney–Rivlin equation:[27,28]

$$\sigma/(\lambda - \lambda^{-2}) = 2C_1 + 2C_2\lambda^{-1} \quad (15)$$

The value of G is given to a good approximation by the relation

$$G = 2C_1 + 2C_2 \quad (16)$$

An accurate measurement of C_1 and C_2, which requires strictly identical conditions (such as sample dimensions), was not possible in the scope of the present experiments.

IV. Experimental Results

We have first tried to establish the influence of the main structural parameters of the network and of the conditions of network formation on the elastic behavior of the networks and on the conformation of the elastic chains in the

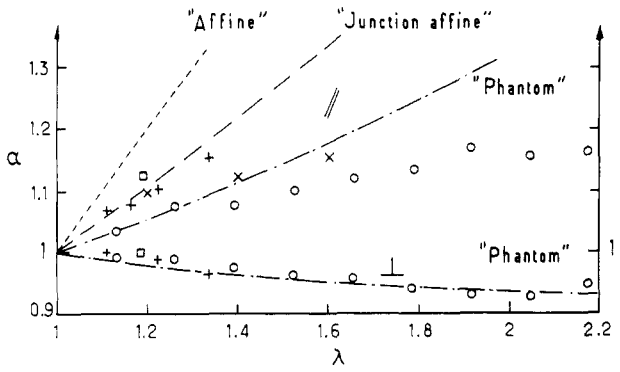

Figure 4. Variation of $\alpha_\parallel$ and $\alpha_\perp$ as a function of λ. Influence of the length of the elastic chains (M_n). The networks were prepared with a constant functionality ($f = 4$) and a constant concentration at network formation ($v_c = 0.71$). (□) $M_n = 3000$; (+) $M_n = 6000$; (×) $M_n = 10\,000$; (○) $M_n = 25\,000$. The lines represent theoretical behaviors.

deformed systems. These parameters are (i) the molecular weight M_n of the PDMS precursor chains (the length of the elastic chains), (ii) the concentration v_c at which the network is formed, and (iii) the functionality f of the cross-links.

Influence of the Length of the Elastic Chains. SANS measurements were carried out on a series of tetra functional networks prepared at a concentration $v_c = 0.71$ with PDMS precursors of different molecular weight (M_n = 3000–25 000). The weight fraction of deuterated species was 20%.

In Figure 4 the experimental values of $\alpha_\parallel$ and $\alpha_\perp$ measured at different deformation ratios are plotted vs. λ. As in Figure 3, the dotted lines are the calculated curves based on the three theoretical models considered. The results obtained clearly show that the type of deformation depends upon the length of the elastic chains: (i) the largest variation of the radius of gyration is observed for the networks containing the shortest chains; (ii) in no case is the deformation of the chains affine in the macroscopic deformation; (iii) the discrepancy between the behavior observed and the affine behavior increases with increasing molecular weight of the network chains.

In the case of the network containing the longest elastic chains ($M_n \simeq 25\,000$), the deformation is even smaller than expected for a phantom network. However, the presence of pendent chains cannot be neglected in this latter case. The weight fraction w_p of pendent chains can be calculated from the amount of extractible polymer. Under the assumption that a macroscopic deformation does not modify the radius of gyration of these pendent chains, the measured radius of gyration is given by

$$R_{g,\parallel m}^2 = w_p R_{g,\parallel i}^2 + (1 - w_p) R_{g,\parallel}^2 \qquad (17)$$

and

$$R_{g,\parallel}^2 = \left(\frac{R_{g,\parallel m}^2 - w_p R_{g,i}^2}{1 - w_p} \right)^{1/2} \qquad (18)$$

The presence of pendent chains also implies a decrease of the cross-link functionality since some functional groups of the cross-links remain unreacted. The resulting average functionality can be easily calculated.

The corrected values of the radius of gyration are very close to those predicted for the phantom network, as shown in Table II.

Influence of Concentration upon Cross-Linking. When networks are prepared with the same precursor polymer but at different polymer concentrations, their mechanical properties can be quite different.

We have studied the influence of v_c on the macroscopic behavior of the networks and on that of the network chains. The networks used in this investigation were prepared with a precursor polymer of molecular weight M_n = 9300 in a concentration range between 0.5 and 1.

Table III shows the experimental values of the moduli measured and, for comparison, the theoretical values calculated on the basis of the junction affine and of the phantom network models (eq 3 and 4). The experimental values are always larger than those calculated in the case of the phantom network. The slight decrease of the calculated values of G results from the small increase of the number of pendent chains as v_c decreases. However, the observed decrease of the experimental values of G with decreasing v_c is far more pronounced. A similar behavior was observed earlier on swollen networks and interpreted as a contribution of the trapped entanglements to the modulus.[29,30] The number of trappped entanglements increases with v_c.

Owing to the SANS technique, it is now possible to check the influence of v_c upon the response of the elastic chains to uniaxial extension. The measurements were performed on samples prepared with three different precursor polymers (M_n = 6000, 10 000, and 25 000) in the bulk and in solution (v_c = 0.60, 0.71, and 1).

The results obtained for the networks prepared with the shortest chains (M_n = 6000) are listed in Table IV. The experimental values of α for samples prepared in the bulk and those corresponding to networks cross-linked in the presence of a solvent ($v_c = 0.71$) can be considered to be identical. In both cases the deformation of the elastic chains is the same as predicted by the junction affine model (displacement of the chain ends affine in the macroscopic deformation).

The experimental data concerning the series of networks prepared with the PDMS precursor of molecular weight

Table II
Variation of $R_{g,\parallel}$ with the Deformation Ratio λ (M_n = 25 000)

λ	$R_{g,\parallel}$,[a] Å	$R_{g,\parallel}$(corr),[b] Å	$R_{g,\parallel}$(phantom),[c] Å $f_e = 3.1$
1	59.6 ± 0.4	59.6	59.6
1.13	61.3 ± 1.2	61.8	61.0
1.26	63.9 ± 1.3	65.1	62.6
1.39	64.1 ± 1.2	65.4	64.3
1.52	65.4 ± 1.0	67.0	66.2
1.65	66.4 ± 0.9	68.3	68.1
1.79	67.3 ± 1.1	69.4	70.3
1.92	69.5 ± 1.0	72.2	72.4
2.05	68.8 ± 1.0	71.3	74.6

[a] Measured values. [b] Values corrected for pendent chains. [c] Expected values for elastic chains in a phantom network with average cross-link functionality $f_e = 3.1$.

Table III
Influence of the Concentration v_c at Network Formation on the Shear Modulus G[a]

v_c	G_{exptl},[b] 10^5 Pa	νRT,[c] 10^5 Pa	$(\nu - \mu)RT$,[d] 10^5 Pa
1	2.03	2.17	0.98
0.90	1.77	2.21	1.01
0.80	1.55	2.19	1.01
0.70	1.26	1.90	0.83
0.60	1.11	1.91	0.83
0.50	0.50	0.88	0.76

[a] Molecular weight of network chains, M_n = 10 000. [b] Experimental values. [c] Calculated values for the junction affine model (eq 3). [d] Calculated values for the phantom network (eq 4).

Table IV
Comparison of Molecular Deformation in Networks Prepared in Solution and in the Bulk[a]

$v_c = 1$			$v_c = 0.71$		
λ	$\alpha_\parallel$	$\alpha_\perp$	λ	$\alpha_\parallel$	$\alpha_\perp$
1.11	1.05 ± 0.4	0.98 ± 0.03	1.11	1.07	1.00
1.22	1.08	0.98	1.16	1.08	
1.33	1.16	0.97	1.22	1.10	0.99
			1.32	1.15	0.96

[a] Molecular weight of network chains, M_n = 6000.

Table V
Comparison of the Molecular Deformation in Networks Prepared in Solution and in the Bulk[a]

	$v_c = 1$		$v_c = 0.71$	$v_c = 0.60$	
λ	$\alpha_\perp$	$\alpha_\parallel$	$\alpha_\parallel$	$\alpha_\parallel$	$\alpha_\perp$
1.11				1.03	0.98
1.12	0.99	1.03			
1.20			1.09		
1.23	0.96	1.05			
1.27				1.05	0.97
1.35	0.95	1.10			
1.37		1.12		1.08	0.89
1.40			1.12		
1.46	0.94	1.15			
1.53	0.95	1.16		1.14	0.93
1.60		1.18	1.15		
1.66	0.93	1.19			
1.70		1.23			
1.78	0.91	1.22			
1.89	0.91	1.25			
1.98	0.89	1.27			

[a] Molecular weight of network chains, M_n = 10 000.

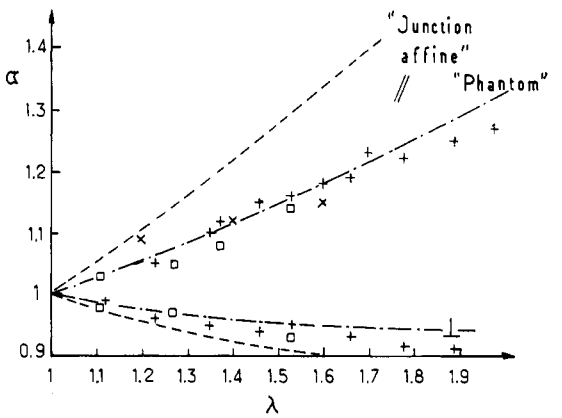

Figure 5. Variation of $\alpha_\parallel$ and $\alpha_\perp$ as a function of λ. Influence of concentration at network formation (v_c). M_n = 9300. (+) v_c = 1; (x) v_c = 0.71; (□) v_c = 0.6.

M_n = 10 000 are gathered in Table V.

In Figure 5 the values of $\alpha_\parallel$ and $\alpha_\perp$ are plotted vs. λ: in this case all the experimental points fit rather well the curve predicted for a phantom network. Thus at the molecular level there is no significant difference in behavior between samples prepared at different concentrations v_c; this contrasts with the noticeable variation of the modulus with v_c (Table VI).

The third series of networks investigated has elastic chains of molecular weight 25 000. In the previous section it was shown that such a network prepared at a concentration v_c = 0.71 behaves like a phantom network in its molecular response to deformation (Figure 4). When the network is prepared in the bulk, the experimental values of α are slightly higher than those predicted for a phantom network but still below the values calculated under the

Table VI
Influence of Concentration v_c on the Shear Modulus[a]

v_c	G_{exptl},[b] 10^5 Pa	νRT,[c] 10^5 Pa	$(\nu - \mu)RT$,[d] 10^5 Pa
1	2.08	2.12	0.97
0.71	1.35	2.06	0.93
0.60	1.08	1.85	0.80

[a] Molecular weight of network chains, M_n = 10 000. [b] Experimental values. [c] Calculated values for the junction affine model (eq 3). [d] Calculated values for the phantom network (eq 4).

Table VII
Molecular Deformation of a Tetrafunctional Network with Long Elastic Chains (M_n = 25 000) Prepared in the Bulk

λ	$\alpha_{\parallel,exptl}$	$[(\lambda^2 + 3)/4]^{1/2}$ [a]	$[(\lambda^2 + 1)/2]^{1/2}$ [b]
1.39	1.13	1.11	1.21
1.51	1.21	1.15	1.28
1.73	1.27	1.23	1.42

[a] Predicted values for the phantom network (eq 11). [b] Predicted values for the junction affine model (eq 8).

Table VIII
Influence of the Concentration v_c on the Shear Modulus of Tetrafunctional Networks Prepared in Solution and in the Bulk[a]

v_c	G_{exptl}, 10^5 Pa	$(\nu - \mu)RT$,[b] 10^5 Pa	νRT,[c] 10^5 Pa
1	0.85	0.32	0.74
0.71	0.48	0.27	0.65

[a] Molecular weight of network chains, M_n = 25 000. [b] Experimental values. [c] Calculated values for the phantom network (eq 4). [d] Calculated values for the junction affine model (eq 3).

hypothesis of the junction affine model (Table VII). Again, we observe the influence of v_c upon the elastic modulus (Table VIII).

Influence of the Functionality of Cross-Links. The last parameter investigated that plays a role in the network behavior is the functionality f of the cross-links. According to the phantom network theory, an increase of the functionality of the cross-links reduces the fluctuations of their average positions. It follows that upon uniaxial stretching the deformation of the elastic chains should be enhanced. On the other hand, the deformation concept proposed by Bastide, which is based upon a disinterpenetration of the elastic chains, also assigns a predominant role to the functionality, since the ratio n/f is proportional to f^{-2} (eq 6). Thus the value of n/f corresponding to a hexafunctional network (with elastic chains of M_n = 10 000) is smaller than that of a tetrafunctional system with shorter chains (M_n = 3100).

We have studied by SANS three hexafunctional networks. In Table IX we have indicated their structural characteristics and listed the corresponding values of $\alpha_\parallel$ and $\alpha_\perp$ measured. In Figure 6 $\alpha_\parallel$ and $\alpha_\perp$ are plotted vs. λ.

We notice that in this case the deformation is larger than would be predicted for a phantom network. Indeed, for these three networks, the molecular deformation is comparable to that of tetrafunctional networks prepared with much shorter network chains (M_n = 3000 and 6000) (Figure 4).

V. Discussion

The comparison between the experimental results and the behavior deduced from theoretical models does not

Table IX
Molecular Deformation in Hexafunctional Networks

M_n = 10 000, υ_c = 1			M_n = 10 000, υ_c = 0.71			M_n = 25 000, υ_c = 1		
λ	$\alpha_\parallel$	$\alpha_\perp$	λ	$\alpha_\parallel$	$\alpha_\perp$	λ	$\alpha_\parallel$	$\alpha_\perp$
1.22	1.11	0.93	1.18	1.08	0.96	1.20	1.10	0.96
1.37	1.19	0.91	1.38	1.17	0.96	1.39	1.16	0.92
						1.45	1.25	0.92

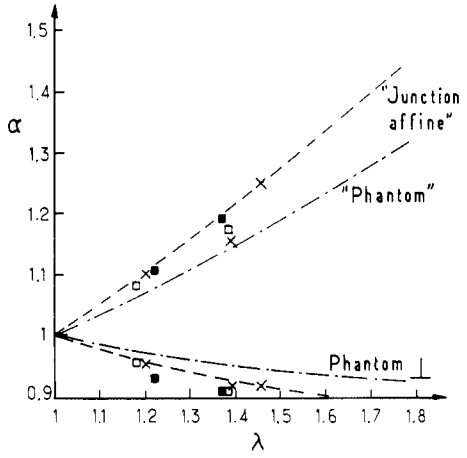

Figure 6. Variation of $\alpha_\parallel$ and $\alpha_\perp$ as a function of λ. Influence of the functionality of the cross-links (f); f = 6): (■) M_n = 10000, υ_c = 1; (□) M_n = 10000, υ_c = 0.71; (x) M_n = 25000, υ_c = 1.

allow an interpretation of the molecular deformation at the level of the mesh size within the framework of a unique model among those proposed by the classical theories of rubber elasticity. Depending upon the length of the elementary chains or on the network functionality, the description of the molecular response is achieved by models taking into consideration more or less accentuated junction fluctuations. The experimental results give clear evidence of the influence of the concentration during the cross-linking process (υ_c) on the elastic modulus whereas at the molecular level, no significant influence of υ_c on the deformation can be detected. As shown by the results obtained on networks with long elastic chains (M_n = 25000), the observed molecular deformation is very low (close to the phantom network behavior), which implies a high degree of mobility of the junction positions. This behavior leads us to the conclusion that during the deformation process, rearrangements of cross-link positions could occur. This process has already been suggested by Bastide:[15] SANS measurements on polystyrene networks submitted to osmotic deswelling showed no significant changes of the dimensions of the network chains over a large range of swelling ratios (between 4 and 18).

Thus, upon deformation, either by swelling or by stretching, the distance between topological neighbors may change less than for phantom networks. The geometrical neighbors (connected by longer paths) can move apart through rearrangements, leading to a more uniform distribution of cross-links. This process does not involve chain deformation and could explain the rather weak response at the molecular level as observed in certain cases by SANS. One can expect that the role played by this type of rearrangement will be the more significant in the case where the number of geometrical neighbors is predominant. In this frame, the characteristic ratio n/f can be proposed as a relevant parameter in the chain deformation mechanism. For this purpose, we have collected in Figure 7 the results of the molecular chain deformation $\alpha_\parallel$ for a series of networks deformed at λ = 1.2 as function of n/f. Again, it can be noticed that the experimental results

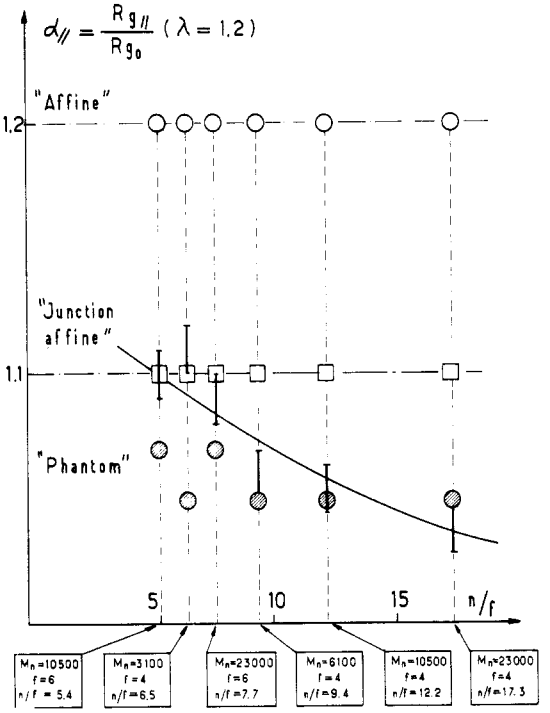

Figure 7. Variation of the elementary chain deformation as a function of the characteristic ratio n/f. Calculated values: (○) affine model; (□) junction affine model; (◯) phantom model. The experimental range is shown by the bar.

cannot be fit with a given unique model of the elasticity theory. However, one observes a continuous decrease of the molecular deformation with increasing values of n/f, attesting that a close correlation exists between this characteristic ratio and the deformation at the level of the network strands.

We can conclude from our experiments that knowledge of the chain deformation at the level of the mesh size of the network does not provide all the necessary information to correlate precisely the molecular processes with the macroscopic response of the network samples. Information about deformation processes occurring at larger scales of distances is required in order to describe more completely the response of the network at the semilocal scale, corresponding to several meshes of the network. For this purpose, SANS experiments on networks with labeled paths through several cross-links are presently in progress.

Acknowledgment. We are grateful to Prof. H. Benoit and Dr. J. Bastide for constructive suggestions and helpful comments. We are also indebted to Dr. P. Rempp for a critical survey of the manuscript. The neutron scattering work was done at the high-flux reactor of the ILL in Grenoble, France. We gratefully acknowledge the material help and advice from the ILL staff.

Registry No. Neutron, 12586-31-1.

References and Notes

(1) Beltzung, M.; Picot, C.; Rempp, P.; Herz, J. *Macromolecules* **1982**, *15*, 1594.
(2) Beltzung, M.; Herz, J.; Picot, C. *Macromolecules* **1983**, *16*, 580.

(3) Flory, P. J. "Principles of Polymer Chemistry"; Cornell University Press: Ithaca, NY, 1953.
(4) Wall, F. T. *J. Chem. Phys.* **1943**, *11*, 527.
(5) Treloar, L. R. C. *Trans. Faraday Soc.* **1943**, *39*, 36.
(6) Flory, P. J.; Rehner, J. *J. Chem. Phys.* **1943**, *11*, 512.
(7) Kuhn, W. *J. Polym. Sci.* **1946**, *1*, 380.
(8) Flory, P. J. *Trans. Faraday Soc.* **1961**, *57*, 829.
(9) James, H. M.; Guth, E. *J. Chem. Phys.* **1943**, *11*, 455.
(10) James, H. M.; Guth, E. *J. Chem. Phys.* **1953**, *21*, 1039.
(11) Flory, P. J. *Proc. R. Soc. London, Ser. A*, **1976**, *351*, 1666.
(12) Graessley, W. W. *Macromolecules* **1975**, *8*, 186.
(13) Flory, P. J. *J. Chem. Phys.* **1977**, *66*, 5720.
(14) Flory, P. J. *Polymer* **1979**, *20*, 1317.
(15) Bastide, J.; Duplessix, R.; Picot, C.; Candau, S. *Macromolecules*, submitted for publication.
(16) Candau, S.; Bastide, J.; Delsanti, M. *Adv. Polym. Sci.* **1982**, *44*, 27.
(17) Bastide, J.; Picot, C.; Candau, S. *J. Macromol. Sci., Phys.* **1981**, *B19*, 13.
(18) Flory, P. J. *Proc. R. Soc. London, Ser. A* **1976**, *351*, 1666.
(19) Belkebir-Mrani, A.; Herz, J.; Rempp, P., *Makromol. Chem.* **1977**, *178*, 485.
(20) Akcasu, A. Z.; Summerfield, G. C.; Jahshan, S. N.; Han, C. C.; Kim, C. Y.; Yu, H. J. *J. Polym. Sci., Polym. Phys. Ed.* **1980**, *18*, 863.
(21) Benoit, H.; Koberstein, J.; Leibler, L. *Makromol. Chem., Suppl.* **1981**, *4*, 85.
(22) Wignall, G. D.; Hendricks, R. W.; Koehler, W. C.; Lin, J. S.; Wai, M. P.; Thomas, E. L.; Stein, R. S. *Polymer* **1981**, *22*, 886.
(23) Boue, F.; Nierlich, M.; Leibler, L. *Polymer* **1982**, *23*, 29.
(24) Duplessix, R. Thesis, Universite Louis Pasteur—Strasbourg, 1975.
(25) Levy, S. Thesis, Universite Louis Pasteur—Strasbourg, 1964.
(26) Pearson, D. S. *Macromolecules* **1977**, *10*, 696.
(27) Mooney, M. *J. Appl. Phys.* **1948**, *19*, 434.
(28) Rivlin, R. S. *Philos. Trans. R. Soc. London, Ser. A* **1948**, *241*, 379.
(29) Belkebir-Mrani, A.; Herz, J.; Beinert, G.; Rempp, P. *Eur. Polym. J.* **1973**, *13*, 277.
(30) Candau, S.; Peters, A.; Herz, J. *Polymer* **1981**, *22*, 1504.

Conformational Characteristics of Poly(vinyl alcohol)†

Romain M. Wolf and Ulrich W. Suter*

Department of Chemical Engineering, Massachusetts Institute of Technology, Cambridge, Massachusetts 02139. *Received June 1, 1983*

ABSTRACT: Conformational energies of *meso*- and *rac*-2,4-pentanediol were estimated, once without account for electrostatic interactions or hydrogen bonds and then with two different electrostatic models for the hydroxyl groups. For the dimer as well as for poly(vinyl alcohol) in aqueous solution, a simple three-state rotational isomeric state model was found. Vicinal NMR coupling constants for the dimer and the characteristic ratio for PVA were computed; they are in excellent agreement with experimental data. In aprotic solutions of the dimer intramolecular hydrogen bond formation is postulated, with an associated free energy of ca. 1 kcal/mol at room temperature.

Introduction

Poly(vinyl alcohol), PVA, is a vinyl polymer of simple structure with a wide range of applications. Commonly used PVA is atactic and usually obtained by radical polymerization of vinyl acetate with subsequent hydrolysis of the side groups.[1] Predominantly isotactic as well as syndiotactic chains can be obtained by a variety of methods.[2,3]

Attempts to characterize atactic PVA in aqueous solution have been many;[4-14] results do not mutually agree very well, however, as will be discussed later. Reliable values for the characteristic ratio of PVA in solution can nevertheless be deduced.[15,16] Heretofore, no satisfactory theory for its conformational characteristics has been presented.

2,4-Pentanediol has often been used as a model compound for PVA.[17-20] The conformational analysis of 2,4-pentanediol has been performed mainly by NMR spectroscopy, and experimental coupling constants have been determined in water as well as in apolar, aprotic solvents.[17-19] In the following, a rotational isomeric state model for PVA in water will be deduced from conformational energy calculations on 2,4-pentanediol. The incidence of intramolecular hydrogen bonds in 2,4-pentanediol and PVA will be discussed in detail.

Conformational Energies

Parameters for the Calculation. The conformational energy was calculated as the sum of intrinsic torsional energy and interaction energies between pairs of nonbonded atoms.

Table I
Parameters Used in Energy Calculations

atom or group	r_i°,[a] Å	α_i,[b] Å^3	N_i[c]
H	1.3	0.42	0.9
C	1.8	0.93	5
O	1.6	0.59	7
CH_3	2.0	1.77	7

[a] Values from ref 44, incremented by +0.1 Å. [b] See ref 29. [c] See ref 27.

The C–C bonds were assigned a 3-fold intrinsic torsional energy function with a barrier $E_{it,C-C}$ = 2.8 kcal/mol.[21] The barrier for the rotation of C–O bonds was derived from experimental data on methanol:[22] A 3-fold, composite rotational barrier of 1.07 kcal/mol has been reported for methanol, and subtraction of van der Waals interactions (between the hydroxyl hydrogen and the methyl hydrogens) yields a barrier of $E_{it,C-O}$ = 0.76 kcal/mol for the 3-fold intrinsic torsional energy function. The reliability of this value was checked by rotational energy calculations for the C–O bond in ethanol: The rotational barrier between antiperiplanar and synclinal conformations is estimated to be 1.13 kcal/mol and is in good agreement with the reported mean experimental value of 1.2 kcal/mol.[23]

Nonbonded interactions between atoms separated by more than two bonds were estimated as described before[24,25] using a spliced, three-piece pair energy function[26] based on the Lennard-Jones function $f_{ij}(d_{ij}) = (a_{ij}/d_{ij}^{12}) - (c_{ij}/d_{ij}^{6})$, d_{ij} being the distance between a pair of atoms

† Dedicated to Professor Walter H. Stockmayer on his 70th birthday.

0024-9297/84/2217-0669$01.50/0